Journal of Fluorine Chemistry 266 (2023) 110084

Contents lists available at ScienceDirect

Journal of Fluorine Chemistry

journal homepage: www.elsevier.com/locate/fluor

Targeted ^{19}F-tags to detect amino acids in complex mixtures using NMR spectroscopy

Keeton Montgomery [a], Aya Elhabashy [a], Guanglin Chen [a], Qiao-Hong Chen [a], V.V. Krishnan [a,b,*]

[a] Department of Chemistry and Biochemistry, California State University, Fresno, CA 93740, USA
[b] Department of Medical Pathology and Laboratory Medicine, University of California Davis School of Medicine, Davis, CA 95616, USA

ARTICLE INFO

Keywords:
Nuclear Magnetic Resonance (NMR)
Fluorine-19
Amino acid
Kinetics
Mixture analysis

ABSTRACT

Nuclear magnetic resonance spectroscopy of fluorine-19 nucleus (^{19}F-NMR) emerges as a powerful tool because of the high sensitivity due to its high natural abundance, broad spectral range, and the simplicity of a spin-half system. However, it is still seldom utilized in the chemistry classroom or research. This article thus aims to demonstrate the power of NMR by investigating the kinetics when a ^{19}F-tag reacts with individual amino acids (AA) and eventually utilizing the approach to identify and quantify various AAs from a complex mixture such as a metabolomics sample. The ^{19}F-tag named 2,5-dioxopyrrolidin-1-yl-2-(trifluoromethyl)benzoate was synthesized following a previously established method. The reaction kinetics of the tag was then continuously measured using ^{19}F NMR in the presence of selected AAs. The estimated reaction rate constants to form the ^{19}F-tags with each AA differ, which could be used as an identification tool. The tag formations were typically completed in 24–48 h in water for all the samples. These demonstrations suggest that ^{19}F-tags could form the basis for chemical kinetics and AA detection using ^{19}F-NMR.

1. Introduction

Nuclear magnetic resonance (NMR) has taken a central role in both education and research, as evidenced by the excellent investigations collected in the four comprehensive volumes by the American Chemical Society Symposium Series [1–4]. Proton (^{1}H) and carbon (^{13}C)-NMR are routinely utilized for structure identification and characterization in research laboratories and industries. In contrast, ^{19}F nucleus is underutilized in the field of NMR, even though the same spectrometer that is used to detect^{1}H- and ^{13}C can perform the experiments for ^{19}F . It is worth noting that the 100% natural abundance of ^{19}F with a high gyromagnetic ratio (3.7 times higher than ^{13}C and 90% of ^{1}H) results in increased sensitivity of the nuclear spin of ½, allowing for a straightforward interpretation of the ^{19}F-NMR spectra [5,6]. In addition to providing reliable quantification similar to ^{1}H NMR, a fluorine nucleus is surrounded by 9 electrons, leading to a broader range of chemical shift dispersion (^{19}F ~350 ppm, in comparison to ^{13}C ~200 ppm, and ^{1}H ~ 12 ppm) and explains the higher sensitivity of fluorine chemical shifts to the local environment. ^{19}F-NMR has also been used in biomolecular applications [7–11] and teaching laboratories [11–13], including structure-activity relationship studies [14].

Identifying and quantifying small molecules, particularly in samples with complex mixtures (e.g., in a metabolomics study), is an emerging area of NMR spectroscopy [15–17]. Amino acids (AA) are among the most valuable metabolites to identify under such criteria because they are vital components in protein synthesis and are crucial for many metabolic reactions [18]. For instance, the abundance of certain AAs (e.g., leucine, alanine, or proline) in plant tissue can serve as abiotic stress factors, including dehydration, osmotic imbalance, or hypersaline soil [18–20]. However, spectral signal overlap among the various AA in complex mixture analysis, such as in metabolomics studies, poses a challenge in identifying and quantifying different AAs. One approach to overcome the challenge is chemically modifying protein amino groups with reactive ^{19}F-tags containing an *N*-hydroxysuccinimide ester (NHS) moiety [21]. The said approach has recently been adopted to modify the AAs [22–24].

This study intends to demonstrate the utilization of one-dimensional ^{19}F NMR spectroscopy in AA identification and quantification. A fluorine tag named 2,5-*dioxopyrrolidin*-1-yl-2-(trifluoromethyl)benzoate was synthesized with accordance to the synthetic procedure established by Chen et al. [23] and used to label the *N*-terminus of the AAs (Fig. 1). A given AA's chemical modification reaction process allows continuous

* Corresponding author at: Department of Chemistry & Biochemistry, California State University, Fresno, CA 93740, USA.
E-mail addresses: krish@csufresno.edu, vvkrishnan@ucdavis.edu (V.V. Krishnan).

https://doi.org/10.1016/j.jfluchem.2022.110084
Received 8 September 2022; Received in revised form 30 December 2022; Accepted 30 December 2022
Available online 31 December 2022

real-time NMR spectral monitoring. Since each AA has a unique side chain, each side chain provides a unique chemical environment that influences the fluorine moiety's chemical shift. This investigation further leverages this technique to measure the rate constants of the reaction of the fluorine tag with a select set of AAs. The rate constants are distinctly different among the different AAs. We aim to provide reliable methodologies for synthesizing the fluorine tag, measuring the reaction kinetics of tag modification of AAs, and quantifying tag-labeled AAs with ^{19}F NMR spectroscopy.

2. Experimental design

2.1. Chemical synthesis and sample preparation

Chemicals: The following chemicals were purchased from Fisher Scientific for direct use in the experiments without further purification. Chemicals used in the synthesis of the ^{19}F-tag: 3-chloro-2-fluorobenzoic acid (CAS: 161,957–55–7, 97%), 2-(trifluoromethyl)benzoic acid (CAS: 433–97–6, 98%), *N*-hydroxysuccinimide (CAS: 6066–82–6, 98+%), and *N,N*'-dicyclohexyl carbodiimide (CAS: 538–75–0, 99%). Solvents, buffers, and reference used in the NMR experiments: Deuterium oxide (CAS: 7789–20–0, 99.95%), potassium phosphate monobasic (CAS: 7778–77–0, 99+%), and acetic acid-d_4 (CAS: 1186–52–3, 99.5%). Amino acids used in the experiments: asparagine (CAS: 70–47–3, 99%), leucine (CAS: 61–90–5, 99%), cysteine (CAS: 52–90–4, 99%), hydroxyproline (CAS: 51–35–4, 99%), and proline (CAS: 609–36–9, 99%).

The general procedure of the experimental approach is illustrated in Fig. 1. First, the ^{19}F-tag (2,5-dioxopyrrolidin-1-yl-2-(trifluoromethyl) benzoate) was prepared by treating 2-(trifluoromethyl)benzoic acid with *N*-hydroxysuccinimide in dichloromethane mediated by DCC (*N, N*'-dicyclohexyl carbodiimide) adhering to the procedure described by Chen et al. [23]. Typically, most NMR experiments require a percentage of the solvent in the form of a deuterated solvent to lock the magnetic field (feedback control of the deuterium NMR signal to keep the resonant frequency adjustment) [25]. The ^{19}F-NMR allows a significant reduction in the need for a D_2O in the sample. Phosphate buffer was prepared in deuterium oxide (99.95%) with potassium phosphate monobasic (90 mM) and trifluoroacetic acid (0.05 mM, chemical shift reference and for quantification). The AAs (individually or in a mixture) were prepared at a pH of 6.8. To demonstrate the utility of the process, five different AAs (asparagine, cysteine, leucine, *trans*-4-hydroxy-proline, and proline) were used both individually and in a mixture. The samples (individual AAs or the mixture) were prepared with a concentration of 0.2 mM with 0.05 mM trifluoroacetic acid (TFA) as the internal standard. In all the experiments, the concentration of the tag is at least six times higher than that of the AA concentrations. The NMR experiments were performed immediately after adding the tag to the sample.

2.2. Kinetic NMR experiments

The NMR experiments were performed in six independent samples: each AA separately and a mixture of AAs (without cysteine). Cysteine was not used in the mix as its reaction rate is much faster than the other AAs (*vide infra*). All ^{19}F-NMR experiments were carried out on a 600 MHz JEOL NMR spectrometer at 30 °C using an HFX-Royal probe.

The qNMR kinetics experiments were performed following the earlier procedure [26]. Each sample was prepared with a small excess volume required for the NMR measurement (~700 μL) in an Eppendorf tube. Next, the ^{19}F-tag was added to the Eppendorf tube, defining the start of the experimental clock ($t = 0$). After a quick mixing of the sample, 600 μL was transferred to an NMR tube. This time difference (delay time) will be added to the first time point when analyzing the data. The kinetic experiments were collected arrayed, with the spectral data saved after a certain number of transients were completed. One-dimensional ^{19}F NMR experiments were acquired at an Ernst angle of 70° [27], which optimizes the signal-to-noise ratio to spin-lattice relaxation time (T_1) when multiple scans are needed. For the kinetic measurements, one-dimensional experiments were conducted in an arrayed manner, with each spectrum in the array taking ~25 min. A total of 256 transients were used for each spectrum, with an acquisition time of ~1.0 s and a relaxation delay of 5.0 s between each transient. Previous work by Chen et al. [7] has established the relaxation time of ^{19}F tagged AAs are less than one second ($1/T_1 = R_1 = 1.16–1.33\ s^{-1}$, and $1/T_2 = R_2 = 1.86–2.0\ s^{-1}$). There a combination of Ernst angle with a relaxation delay of 6 s can be considered sufficient for quantification of the ^{19}F-NMR peak intensities with a high accuracy. The kinetic experiments are typically performed for 24 h to monitor the completeness of the reactions, with some experiments taking up to 48 h.

2.3. Analysis of kinetic NMR experimental data

Time domain NMR data were processed using MestReNova® using a standard procedure (zero-filled once with a sine-squared apodization and baseline correction). All the spectra were referenced using TFA at −76.55 ppm. Based on the TFA peak area, the concentration of the AAs indirectly estimated as

$$[AA] = \frac{I_{AA}}{I_{TFA}} \times \frac{N_{TFA}}{N_{AA}} \times [TFA] \quad (1)$$

where [TFA] is the concentration of TFA, and I_{AA} is the peak area of the AA of interest, with N_{TFA} and N_{AA} are the number of fluorine nuclei of TFA and the AAs, respectively.

First, all the kinetics measurements of product formation were subjected to an initial rate estimation (linear region of the curve). Then, the mechanism of formation of tagged AA is assumed to be a bimolecular reaction with one molecule of the ^{19}F-tag reacting with one molecule of the AA to form the ^{19}F-tagged AA (^{19}FAA); The formation of the ^{19}F-tagged AAs generally requires a second-order rate equation ($[^{19}F - tag] + [AA] \rightarrow [^{19}FAA]$) (rate-constant in units of $M^{-1}s^{-1}$).

$$-\frac{d}{dt}[AA] - \frac{d}{dt}[^{19}F - tag] = \frac{d}{dt}[^{19}FAA] = k[AA][^{19}F - tag] \quad (2)$$

Since the concentration of tag was excess (concentration of amino acids used was less than one-sixth of that of tag 2) $[AA] \ll [^{19}F - tag]$, the product $k[^{19}F - tag]$ can be considered as a constant, thus simplifying the second-order reaction (Eq. (2)) to a pseudo-first-order response (Eq.

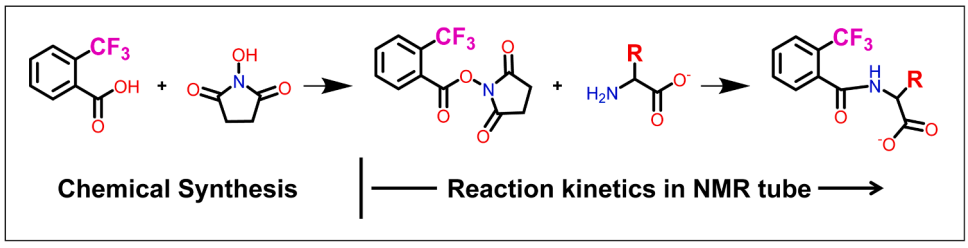

Fig. 1. Experimental design. The first part of the investigation is the organic synthesis of the ^{19}F-tag. Next, the reaction kinetics of the tag with the amino acids is monitored in real-time by ^{19}F -NMR. The 'R' stands for any amino acid side chain.

(3)).

$$-\frac{d}{dt}[AA] = k'[AA] \quad (3)$$

The pseudo-first-order rate constant $k' = k[^{19}F - tag]_0$ in the units of s^{-1}, with $[^{19}F - tag]_0$ the tag concentration at $t = 0$. Since the tag concentration was in excess, the formation of the backbone amide product can be regarded as a pseudo-first-order reaction. Therefore, the observed formation of the ^{19}F-AA as a function of time for this pseudo-first-order process can be written as

$$\left[^{19}\mathrm{F} - \mathrm{AA}\right](t) = \left[^{19}\mathrm{F} - \mathrm{AA}\right]_{eq}\left(1 - e^{-k't}\right) \quad (4)$$

In Eq. (4), $[^{19}$F-AA$]_{eq}$ is the concentration of the ^{19}F-tagged AAs when the reaction is complete ($t >> 0$). Once the concentration of the ^{19}F-AA is obtained from NMR spectra Eqs. (1), (4) can be utilized to estimate the rate constants using a non-linear least square fitting procedure. Using the initial concentration of the ^{19}F-tag, a second-order rate was calculated (second-order rate constant = k/[^{19}F-tag] in $M^{-1}s^{-1}$).

For amino acids with other functional groups, such as cysteine, the reaction kinetics tends to be more complex than the pseudo-first-order mechanism (Eq. (4)). Therefore, this paper did not analyze the kinetics data of cysteine tag formation. The data analysis and plots were generated using Microsoft Excel and the R statistical environment [28].

3. Results and discussion

3.1. ^{19}F-NMR of tagged AAs

Our one-dimensional ^{19}F-NMR experiments indicate that the reactions of the different AAs with the fluorine tag required different lengths of time to complete. Fig. 2 shows the spectra of all five ^{19}F-labeled AAs at the end of the reaction. The chemical shifts of the individual ^{19}F-labeled AA are distinguishable in each spectrum: Cystine (−58.42 ppm), cysteine (−59.05 ppm), asparagine (Asn, −59.09 ppm), leucine (Leu, −59.22 ppm), hydroxy-proline (Hyp, −59.92 ppm) and proline (Pro, −60.60 ppm). Proline and hydroxy-proline residues indicate the existence of other minor products at −60.27 ppm and −60.36 ppm, respectively. The area under the curve from both the major and minor peaks was considered when we estimated the concentration of these two ^{19}F-labeled AAs. All the spectra showed the ^{19}F peak for the hydrolysis product (−59.73 ppm), except for the reaction with cysteine, where the reactant was fully converted to the product.

3.2. Reaction monitoring of ^{19}F-tagged AAs individually

Product formation of the ^{19}F-labeled arginine, leucine, hydroxy-proline and proline are included in the supporting information (Fig. S1). An initial rate (linear region of the product formation, < 5 hrs.) and pseudo-first-order analyses were performed. Table 1 summarizes the results when the pseudo-first-order rates are converted to a second-order rate constant using the initial concentration of the ^{19}F-tag (initial concentration 1.2 mM). The second-order rate constant of ^{19}F-leucine is the fastest (33.61 ± 1.23 $mM^{-1}s^{-1}$), while the ^{19}F-hydroxy-proline is the slowest (35.86 ± 2.04 $mM^{-1}s^{-1}$). The rate constants, however, do not show a large variation (31.99 $mM^{-1}s^{-1}$ to 38.22 $mM^{-1}s^{-1}$), suggesting that within the experimental time, the reaction is completed for all the amino acids.

The progress of the conversion from cysteine to ^{19}F-labeled cysteine is shown in Fig. 3. The internal reference TFA stays constant during the entire process of the experiment as the ^{19}F-tag converts to the ^{19}F-labeled cysteine (Fig. 3). An intermolecular interaction between the ^{19}F-labeled cysteine produced in the reaction continues to form the disulfide bridge to form the ^{19}F-labeled cystines [29]. The tagged cysteine concentration reduces over time due to the gradual formation of cystine. The sulfur moiety in cysteine rapidly forms the unstable thioester

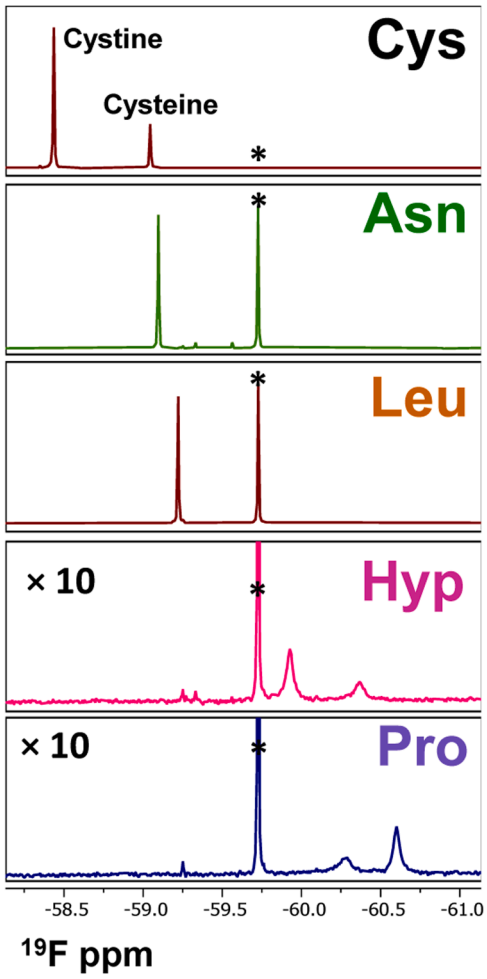

Fig. 2. ^{19}F-NMR spectra of the ^{19}F-labeled amino acids that were acquired when the reactions were complete. The three-letter amino acid codes correspond to Cys: cysteine/cystine, Asn: asparagine, Leu: leucine, Hyp: hydroxy-proline, and Pro: proline. The peak position of the ^{19}F -hydrolysis product is marked by "*'.

Table 1
Kinetics of ^{19}F-AA formation.

Amino Acid	Individually Rate ($mM^{-1}s^{-1}$)	Mixture Rate ($mM^{-1}s^{-1}$)
Asparagine (Asn)	31.99 ± 1.18	59.68 ± 1.64
Leucine (Leu)	33.61 ± 1.23	56.64 ± 1.48
Hydroxy-proline (Hyp)	35.86 ± 2.04	77.11 ± 2.96
Proline (Pro)	38.22 ± 2.13	52.75 ± 1.64

product, followed by the displacement of cysteine to create the amide product. With time, the cystine amide product is formed. A difference in the chemical shift differences between ^{19}F-labeled cysteine (−59.05 ppm) and ^{19}F-labeled cystine (−58.42 ppm) enables tracking the two products from the same data. As the formation of ^{19}F-cysteine/cystine does not follow the proposed pseudo-first order reaction mechanism, rate constants were not estimated.

3.3. Reaction monitoring of ^{19}F-tagged AAs in a mixture

The application of the ^{19}F-tag to identify individual AA in the mixture is demonstrated by performing the reaction of the ^{19}F tag with a mixture of AAs (except cysteine). Fig. S2 shows the mixture's corresponding spectra where the ^{19}F-tagged AA's chemical shifts closely

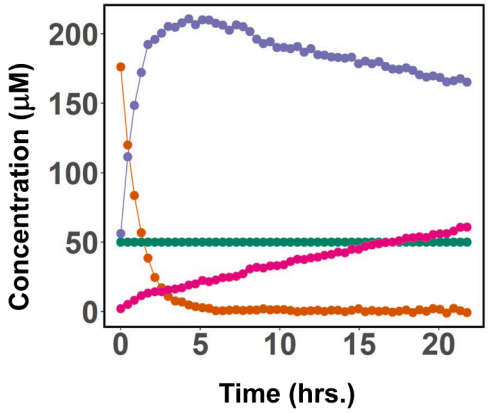

Fig. 3. Reaction progress monitoring by ^{19}F-NMR of ^{19}F-labeled cysteine. The time-dependent change in the various signals when ^{19}F -tag was reacted with amino acid cysteine. The decay of the reactant thioester product leads first to the formation of the product ^{19}F-labeled cysteine, which converts into cystine due to the disulfide formation of the cysteines. The concentration of trifluoroacetic acid (TFA) used as a reference remains constant during the reaction.

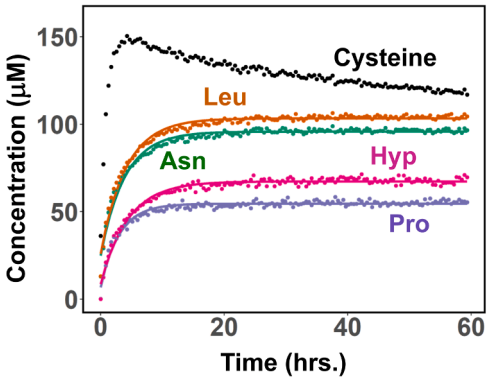

Fig. 4. Reaction monitoring of ^{19}F -tagged amino acids. Real-time tracking of the ^{19}F -tagged amino acids formed when the ^{19}F tag was added to the mixture of amino acids: Cysteine/cystine, Asn: asparagine, Leu: leucine, Hyp: hydroxy-proline, and Pro: proline. The experimental values (shown as symbols) are fit to an exponential growth function based on a pseudo-first-order reaction.

match those obtained individually (Fig. 1). The real-time monitoring of the ^{19}F-tagged AAs is shown in Fig. 4. An initial rate estimation of the ^{19}F-tag formation is also summarized in supporting information (Fig. S3). The analysis results in the following rate constants: Asn (22.05 ± 2.46 mM/hr.), Leu (22.97 ± 2.78 mM/hr.), Hyp (15.98 ± 1.64 mM/hr.), and Pro (16.44 ± 1.71 mM/hr.). A pseudo-first order analysis on the mixture of the AAs is the formation rate of each AA in the mix presented as a second order rate is Asn (59.68 ± 1.64 $mM^{-1}s^{-1}$), Leu (56.64 ± 1.48 $mM^{-1}s^{-1}$), Hyp (77.11 ± 2.96 $mM^{-1}s^{-1}$), and Pro (52.75 ± 1.64 $mM^{-1}s^{-1}$).

Even though the result for the ^{19}F-tagged cysteine is included in Fig. 4, the rate is not estimated due to the formation of the secondary reaction product (cystine). The reaction rate for each AA in the mixture is generally faster than the corresponding one for the individual AA, but the overall trend to equilibrium is the same (Table 1). The ^{19}F-tagged cysteine/cystine reaction rate is much faster than other ^{19}F-tagged AAs. These results suggest that the signature chemical shifts of each ^{19}F-tagged AA and the rate of converting each AA to its ^{19}F-tagged product can be used to identify the AAs in a complex mixture. The AA peaks were identified with reference to spectral chemical shifts of the amide product for individually tagged AAs ran at a pH of 6.8. Side chain and amide products of lysine, cysteine, and histidine were distinguished by comparing our chemical shifts with those obtained by Chen et al. [23]. The ^{19}F-tagged cysteine signal is much more intense than the rest in the mixture due to the greater nucleophilic capability of cysteine.

Intriguingly, the chemical shifts of the ^{19}F-tagged AAs identified in this work at pH 6.8 did not reproduce those reported by Chen et al. at pH 7.5, suggesting that different pH values affect the chemical shits of amide-containing compounds [23]. The pH-dependent chemical shifts for ^{19}F-tagged AAs have been reported by Huang et al. [24]. Therefore, it is crucial to use an appropriate pH-adjusted buffer to ensure the chemical shifts in the specific sample are not altered from standard data collected at a given sample pH.

4. Conclusion

Considering AAs form a significant subset of metabolites, a proof-of-concept study has been investigated to develop a method for AA identification and quantification using one-dimensional ^{19}F NMR spectroscopy. The work presented here elucidates a repeatable, feasible technique that can be implemented in laboratories interested in quantifying ^{19}F-tagged AAs using ^{19}F NMR spectroscopy. In addition, utilizing ^{19}F-NMR spectroscopy enables tracking single peaks representing one amino acid instead of many, thus possibly eliminating error. Further, this work exemplifies a method of AAs quantification in complex mixtures, namely for metabolomics. For example, identifying specific chemical shifts with broad pH ranges can aid in developing libraries and programs intended for AA quantification around this method.

Declaration of Competing Interest

The authors declare that they have no known competing financial interests or personal relationships that could have appeared to influence the work reported in this paper.

Acknowledgments

This work was partly supported by the SC3 NIH grant (GM125546). The 600 MHz NMR spectrometer was funded by NSF MRI (1919908)

Supplementary materials

Supplementary material associated with this article can be found, in the online version, at doi:10.1016/j.jfluchem.2022.110084.

References

[1] D. Soulsby, L.J. Anna, A.S. Wallner, NMR spectroscopy in the undergraduate curriculum, in: Volume 4: In-Person and Distance Learning Approaches, 1376, 2021.
[2] D. Soulsby, L.J. Anna, A.S. Wallner, NMR Spectroscopy in the Undergraduate Curriculum: Upper-Level Courses and Across the Curriculum Volume 3, 1225, 2016.
[3] D. Soulsby, L.J. Anna, NMR Spectroscopy in the Undergraduate Curriculum: first Year and Organic Chemistry Courses Volume 2 1221 (2016).
[4] D. Soulsby, L.J. Anna, NMR Spectroscopy in the Undergraduate Curriculum: first Year and Organic Chemistry Courses Volume 2 1128 (2013).
[5] Dolbier Jr, W., Guide to Fluorine NMR For Organic Chemists. 2009, Hoboken, NJ.
[6] J.X. Yu, et al., New frontiers and developing applications in 19F NMR, Prog. Nucl. Magn. Reson. Spectrosc. 70 (2013) 25–49, https://doi.org/10.1016/j.pnmrs.2012.10.001.
[7] H. Chen, et al., 19F NMR: a valuable tool for studying biological events, Chem. Soc. Rev. 42 (20) (2013) 7971–7982, https://doi.org/10.1039/c3cs60129c.
[8] M.A. Danielson, J.J. Falke, Use of 19F NMR to probe protein structure and conformational changes, Annu. Rev. Biophys. Biomol. Struct. 25 (1996) 163–195, https://doi.org/10.1146/annurev.bb.25.060196.001115.
[9] J.L. Kitevski-LeBlanc, R.S. Prosser, Current applications of 19F NMR to studies of protein structure and dynamics, Prog. Nucl. Magn. Reson. Spectrosc. 62 (2012) 1–33, https://doi.org/10.1016/j.pnmrs.2011.06.003.
[10] D. Rose-Sperling, et al., 19F NMR as a versatile tool to study membrane protein structure and dynamics, Biol. Chem. 400 (10) (2019) 1277–1288, https://doi.org/10.1515/hsz-2018-0473.
[11] M. Druelinger, D. Dillon, Using 19F NMR spectra to enhance undergraduate organic teaching and research labs. **NMR** Spectroscopy in the Undergraduate

Curriculum, Volume 4: In-Person and Distance Learning Approaches, American Chemical Society, 2021, pp. 151–174, 978-0-8412-9850-7.
[12] D.J. deMendonca, et al., Structure determination using 19F NMR: a simple fluorination experiment of cinnamyl alcohol, J. Chem. Educ. 72 (8) (1995) 736, https://doi.org/10.1021/ed072p736.
[13] S.K. Bur, et al., Fragment-based ligand discovery using protein-observed 19F NMR: a second semester organic chemistry CURE project, J. Chem. Educ. 98 (6) (2021) 1963–1973, https://doi.org/10.1021/acs.jchemed.1c00028.
[14] A. Divakaran, S.E. Kirberger, W.C.K. Pomerantz, SAR by (Protein-Observed) 19F NMR, Acc. Chem. Res. 52 (12) (2019) 3407–3418, https://doi.org/10.1021/acs.accounts.9b00377.
[15] H.K. Kim, Y.H. Choi, R. Verpoorte, NMR-based plant metabolomics: where do we stand, where do we go? Trends Biotechnol. 29 (6) (2011) 267–275, https://doi.org/10.1016/j.tibtech.2011.02.001.
[16] M. Pérez-Trujillo, T.J. Athersuch, Special Issue: NMR-based metabolomics, Molecules 26 (11) (2021), https://doi.org/10.3390/molecules26113283.
[17] D.S. Wishart, NMR metabolomics: a look ahead, J. Magn. Reson. 306 (2019) 155–161, https://doi.org/10.1016/j.jmr.2019.07.013.
[18] M. Trovato, et al., Editorial: amino acids in plants: regulation and functions in development and stress defense, Front. Plant Sci. (2021) 12.
[19] J.F. Dufayard, et al., New insights on leucine-rich repeats receptor-like kinase orthologous relationships in angiosperms, Front. Plant Sci. 8 (2017) 381, https://doi.org/10.3389/fpls.2017.00381. -381.
[20] E. Socha, M. Koba, P. Kośliński, Amino acid profiling as a method of discovering biomarkers for diagnosis of neurodegenerative diseases, Amino Acids 51 (3) (2019) 367–371, https://doi.org/10.1007/s00726-019-02705-6.
[21] G.T. Hermanson, Bioconjugate Techniques, Academic press, 2013, 0123822408.
[22] Y.T. Chen, et al., Simultaneous discrimination and quantification of enantiomeric amino acids under physiological conditions by chiral 19F NMR tag, Anal. Chem. 94 (22) (2022) 7853–7860, https://doi.org/10.1021/acs.analchem.2c00218.
[23] Y.T. Chen, et al., Simultaneous identification and quantification of amino acids in biofluids by reactive 19F-tags, Chem. Commun. 57 (97) (2021) 13154–13157, https://doi.org/10.1039/D1CC05060E.
[24] B. Huang, et al., Simultaneous analysis of amino acids based on discriminative 19F NMR spectroscopy, Bioorg. Chem. 124 (2022), 105818, https://doi.org/10.1016/j.bioorg.2022.105818.
[25] P.C.M. van Zijl, The use of deuterium as a nucleus for locking, shimming, and measuring NMR at high magnetic fields, J. Magn. Reson. (1969) 75 (2) (1987) 335–344, https://doi.org/10.1016/0022-2364(87)90039-4.
[26] J.Y. Vang, et al., Enzyme kinetics by real-time quantitative NMR (qNMR) spectroscopy with progress curve analysis, Anal. Biochem. 658 (2022), 114919, https://doi.org/10.1016/j.ab.2022.114919.
[27] R.R. Ernst, W.A. Anderson, Application of fourier transform spectroscopy to magnetic resonance, Revi. Sci. Instrum. 37 (1) (1966) 93–102, https://doi.org/10.1063/1.1719961.
[28] Team, R.D.C., R: a language and environment for statistical computing. 2009, R Foundation for Statistical Computing.: Vienna, Austria.
[29] R.J. Dougherty, J. Singh, V.V. Krishnan, Kinetics and thermodynamics of oxidation mediated reaction in L-cysteine and its methyl and ethyl esters in dimethyl sulfoxide-d6 by NMR spectroscopy, J. Mol. Struct. 1131 (2017) 196–200, https://doi.org/10.1016/j.molstruc.2016.11.038.